Atomic Force Microscopy Imaging and Electrical Recording of Lipid Bilayers Supported over Microfabricated Silicon Chip Nanopores: Lab-on-a-Chip System for Lipid Membranes and Ion Channels

Arjan P. Quist,[†,‡] Ami Chand,[§] Srinivasan Ramachandran,[†] Chiara Daraio,[||] Sungho Jin,[||] and Ratnesh Lal*[,†]

Neuroscience Research Institute, University of California, Santa Barbara, California 93106, Applied NanoStructures Inc., 1700 Wyatt Drive, Suite 5, Santa Clara, California 95054, and Department of Mechanical and Aerospace Engineering, University of California at San Diego, La Jolla, California 92093

Received July 25, 2006. In Final Form: October 15, 2006

We describe a silicon chip-based supported bilayer system to detect the presence of ion channels and their electrical conductance in lipid bilayers. Nanopores were produced in microfabricated silicon membranes by electron beam lithography as well as by using a finely focused ion beam. Thermal oxide was used to shrink pore sizes, if necessary, and to create an insulating surface. The chips with well-defined pores were easily mounted on a double-chamber plastic cell recording system, allowing for controlling the buffer conditions both above and below the window. The double-chamber system allowed using an atomic force microscopy (AFM) tip as one electrode and inserting a platinum wire as the second electrode under the membrane window, to measure electrical current across lipid bilayers that are suspended over the pores. Atomic force imaging, stiffness measurement, and electrical capacitance measurement show the feasibility of supporting lipid bilayers over defined nanopores: a key requirement to use any such technique for structure−function study of ion channels. Online addition of gramicidin, an ion-channel-forming peptide, resulted in electrical current flow across the bilayer, and the $I-V$ curve that was measured using the conducting AFM tip indicates the presence of many conducting gramicidin ion channels.

Introduction

Ion channels are proteins in cell membranes that act as pores with the ability to open or close in response to specific stimuli. This allows for gating of ions in and out of the enclosed subcellular compartments and whole cells. Traditionally, single-channel ion currents are studied using the patch-clamp technique,[1,2] in which a glass pipet filled with electrolyte is used to contact the membrane surface and measure ionic current. Recently, there has been a growing interest in chip-based patch clamping, using planar silicon microstructures. The aperture in a planar chip device has a lower background noise due to small series resistance and capacitance,[3] and the planar chip layout allows in situ measurements using atomic force microscopy (AFM) or fluorescence microscopy simultaneous with the electrical recording. However, these systems use whole cells that are too mobile to be useful for AFM imaging of ion channels at molecular resolution. Also, micrometer-sized pores may be too large for high-resolution imaging of reconstituted ion channels in bilayers. For such a study, a supported bilayer system with defined nanopores would be a more feasible option. Furthermore, traditional techniques are laborious and require precisely pulled pipets that need to be positioned at the membrane interface using micromanipulators.

Several silicon wafer-based patch-clamp systems have been designed and tested. Macroscopic ion channel activities in whole-cell systems have been studied using ion-track etching of planar, microstructured glass substrates.[3] Similarly, oocytes were patch-clamped to micromachined poly(dimethylsiloxane) (PDMS) substrates.[4] Silicon devices are perhaps the most versatile option to investigate single-channel conductance, although other chip-based patch-clamp devices were proposed using silicon oxide-coated nitride membranes,[5] polyimide films,[6] and quartz substrates.[7] To mimic the traditional patch pipets, a silicon oxide micronozzle was developed,[8] though no channel activity was observed due to a low electrical seal. Macroscopic channel activity has been observed using a silicon wafer-based device.[9] To improve the seal resistance, Teflon was deposited on silicon pores to produce a hydrophobic surface for bilayer attachment.[10] A multiple planar patch-clamp system has been designed that uses lateral cell trapping junctions to reduce capacitive coupling and allows for multiplexed parallel patch sites.[11]

However, these techniques do not give information about the 3D conformational states of ion channels related to their activity. Thus, the need exists for techniques that can image the structural features of ion channels and recording their electrical activity simultaneously. For instance, transport of calcium ions through hemichannels has been demonstrated using AFM imaging on the whole-cell level,[12] while the conformational differences

* To whom correspondence should be addressed at the Center for Nanomedicine, Department of Medicine, University of Chicago, Chicago, IL 60637. Phone: (773) 702-2263. E-mail: rlal@uchicago.edu.

† University of California, Santa Barbara.

‡ Present address: Richmond Chemical Corp., 2210 Midwest Rd., Oak Brook, IL 60523.

§ Applied NanoStructures Inc.

|| University of California at San Diego.

(1) Neher, E.; Sakmann, B. *Nature* **1976**, *260*, 799−802.

(2) Sakmann, B.; Neher, E. *Single Channel Recording*; Plenum: New York, 1983.

(3) Fertig, N.; Klau, M.; George, M.; Blick, R. H.; Behrends, J. C. *Appl. Phys. Lett.* **2002**, *81*, 4865−4867.

(4) Klemic, K. G.; Klemic, J. F.; Reed, M. A.; Sigworth, F. J. *Biosens. Bioelectron.* **2002**, *17*, 597−604.

(5) Fertig, N.; Tilke, A.; Blick, R. H.; Kotthaus, J. P.; Behrends, J. C.; ten Bruggencate, G. *Appl. Phys. Lett.* **2000**, *77*, 1218−1220.

(6) Stett, A.; Bucher, V.; Burkhardt, C.; Weber, U.; Nisch, W. *Med. Biol. Eng. Comput.* **2003**, *41*, 233−240.

(7) Fertig, N.; Blick, R. H.; Behrends, J. C. *Biophys. J.* **2002**, *82*, 161A−161A.

(8) Lehnert, T.; Gijs, M. A. M.; Netzer, R.; Bischoff, U. *Appl. Phys. Lett.* **2002**, *81*, 5063−5065.

(9) Pantoja, R.; Nagarah, J. M.; Starace, D. M.; Melosh, N. A.; Blunck, R.; Bezanilla, F.; Heath, J. R. *Biosens. Bioelectron.* **2004**, *20*, 509−517.

(10) Wilk, S. J.; Goryll, M.; Laws, G. M.; Goodnick, S. M.; Thornton, T. J.; Saraniti, M.; Tang, J.; Eisenberg, R. S. *Appl. Phys. Lett.* **2004**, *85*, 3307−3309.

10.1021/la062187z CCC: $37.00
Published on Web 12/08/2006

between open and closed hemichannels were imaged using AFM after reconstitution of hemichannels in lipid bilayers.[13] Similarly, AFM has been successfully used to study the 3D structure of several types of amyloid ion channels related to protein misfolding disease.[14,15] However, a direct correlation of the 3D structure and activity of single ion channels is yet to be demonstrated. To show the real-time transport of ions through ion channels while simultaneously imaging their open and closed 3D structural conformations, conductive AFM can potentially be used. This technique was previously used to image the conductivity of polymer blends.[16]

Here we report on the fabrication of nanopores in silicon membranes that could be used for supported bilayer study with two fluid compartments, one each below and above the channels. These silicon chips with nanopores support reconstituted lipid bilayers; lipid bilayers are stiff enough for allowing their imaging with AFM. Using conducting AFM tips, bulk electrical current could be recorded for a population of ion channels formed in the lipid bilayer and over the chip nanopores by online addition of gramicidin, an ion-channel-forming peptide.

Materials and Methods

Two approaches were used to produce nanopores.

First, as an initial test, pores were produced in 200 nm thick silicon nitride windows (SPI Supplies, West Chester, PA) using electron beam lithography combining arrays of pores of varying sizes with large markers to be easily located by optical microscopy for easier navigation of the AFM tip to the pores. Patterning was performed using a Jeol JBX 5DII system (Jeol, Peabody, MA) with an LaB6 electron source at a 50 kV acceleration voltage and a 50−100 pA current and ZEP520 as a high-resolution resist. After development of the patterns in 100% amyl acetate, a Bosch deep reactive ion etch was used to etch the pores through the silicon nitride windows. After final stripping of the resist and cleaning using acetone, isopropyl alcohol, and water successively, images of the pores were obtained by scanning electron microscopy (SEM; FEI, Hillsboro, OR) as well as AFM (Veeco Metrology, Santa Barbara, CA). For imaging of nanopores in air ACT silicon cantilevers (Applied NanoStructures, Santa Clara, CA) were used with a spring constant of 48 N/m and a resonance frequency of 330 kHz (tip radius estimated as less than 10 nm). In liquids, silicon nitride cantilevers (NPS) (Digital Instruments, Santa Barbara, CA) were used with a spring constant of 0.06 N/m and operating frequencies for the tapping mode around 8 kHz (tip radius estimated as around 25 nm). Scanning rates varied from 0.3 to 2 Hz.

Second, silicon membranes were used. They were microfabricated using silicon-on-insulator (SOI) wafers. As shown in Figure 1A the SOI wafer consists of a device layer, a buried oxide layer, and a handle wafer of thicknesses 0.34, 0.3, and 300 μm, respectively. A thermal oxide of 300 Å thickness was deposited, followed by a 1000 Å low-stress low-pressure chemical vapor deposition (LPCVD) of silicon nitride. These layers function as masking layers for etching silicon in a KOH solution. A photolithography step was performed to open a window in the silicon nitride and oxide layers to expose the silicon wafer for etching as shown in Figure 1B. Wafers were then etched using 33% aqueous KOH solution at 70 °C to produce arrays of dies 7 mm × 7 mm in size, each having a pyramidal shaped opening of 200 μm × 200 μm in the center. Etching was stopped at the buried oxide layer, thus leaving an oxide and Si membrane window. The wafer after this step is shown in Figure 1C, and an SEM image of the wafer's backside with the pyramid-shaped opening is shown in Figure 1E. The LPCVD silicon nitride layer was removed in hot phosphoric acid. The oxide layers were stripped in buffered hydrofluoric acid (HF), leaving a silicon membrane. The dies were processed using a dual-beam focused ion beam (FIB) (FIB International, Santa Clara, CA), creating one nanopore, 70−150 nm in diameter, through the Si membrane in each die. A 70 nm diameter pore is shown in Figure 1F. To provide electrical insulation, thermal oxide of various thicknesses was grown on both the top and bottom sides of the die using plasma-enhanced chemical vapor deposition (PECVD). The final structure is shown in Figure 1D.

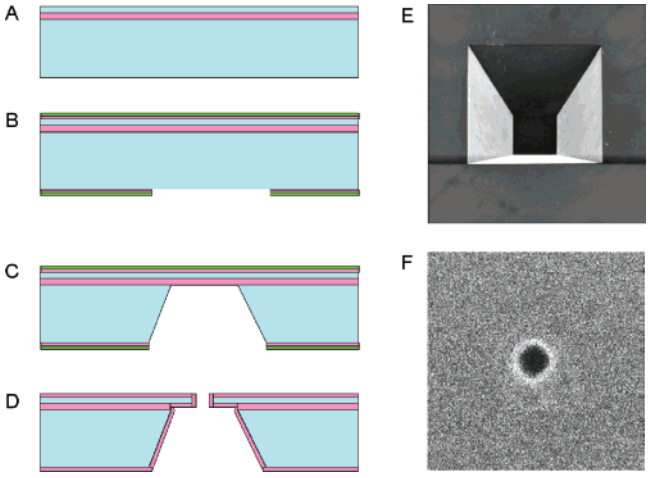

Figure 1. Fabrication procedure: (A) device layer (blue), buried oxide layer (pink), and handle wafer (blue); (B) thermal oxide and silicon nitride (green) added as a masking layer; (C) photolithography leaves an etched pyramid-shaped pit; (D) Removal of masking layers and nanopore fabrication using FIB followed by oxide deposition (for details see the text); (E) the backside of the wafer after etching shows a 200 × 200 μm pyramidal opening; (F) nanopore created by FIB, diameter 70 nm.

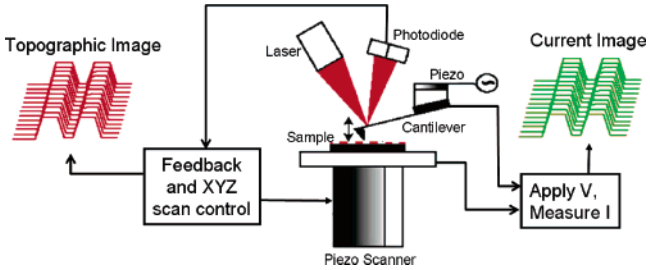

Figure 2. Schematic setup of AFM imaging and combined electrical recording. Images of topography and current are acquired simultaneously.

Nanopore membranes were mounted on specially designed plastic liquid cells to exchange fluid above or below the membrane. $I-V$ curves were obtained in 135 mM KCl solution. Current was measured using the conductive AFM setup with the cantilevered tip holder as an electrode on the top and a reference electrode under the pore chip (Figure 2). For conductance AFM, contact mode silicon cantilevers (spring constant of 0.2 N/m, model no. ANSCM-PC, Applied NanoStructures) with a conductive coat of 3 nm of titanium and 25 nm of platinum were used at a resonance frequency of 11 kHz. The tip radius was estimated at less than 50 nm. In the absence of an insulating coat, when buffer is present on both sides of the chip, current is measured through the complete tip holder clip. To image current flow between the AFM tip and single nanopore in the silicon chip, 135 mM KCl solution was placed only under the pore chip and a flow of humid air was maintained over the top surface. This setup ensured that, by allowing only a local water meniscus contact between

(11) Seo, J.; Ionescu-Zanetti, C.; Diamond, J.; Lal, R.; Lee, L. P. *Appl. Phys. Lett.* **2004**, *84*, 1973−1975.
(12) Quist, A. P.; Rhee, S. K.; Lin, H.; Lal, R. *J. Cell Biol.* **2000**, *148*, 1063−1074.
(13) Thimm, J.; Mechler, A.; Lin, H.; Rhee, S.; Lal, R. *J. Biol. Chem.* **2005**, *280*, 10646−10654.
(14) Lin, H.; Bhatia, R.; Lal, R. *FASEB J.* **2001**, *15*, 2433−2444.
(15) Quist, A.; Doudevski, L.; Lin, H.; Azimova, R.; Ng, D.; Frangione, B.; Kagan, B.; Ghiso, J.; Lal, R. *Proc. Natl. Acad. Sci. U.S.A.* **2005**, *102*, 10427−10432.
(16) Ionescu-Zanetti, C.; Mechler, A.; Carter, S. A.; Lal, R. *Adv. Mater.* **2004**, *16*, 385−389.

the conducting AFM tip and the sample, only the local conductance through each pore was measured.

AFM was also used to image pores after deposition of lipid vesicles of 1,2-dioleoyl-*sn*-glycero-3-phosphocholine (DOPC; Avanti Polar Lipids, Alabaster, AL) prepared by a previously described method.[17] Briefly, vesicles were formed by drying 1 mg of DOPC lipid in a glass tube, kept in a desiccator overnight, and rehydrated in buffer with occasional vortexing. Lipid vesicles were several hundred nanometers and larger in diameter. For vesicle deposition onto the silicon chip with a nanopore, a droplet (50 μL, 1 mg/mL) of vesicles was placed on the pore chip, allowed to adsorb for 30 min, and rinsed with buffer.

For conductance AFM imaging after bilayer deposition, experiments were performed in a liquid cell to avoid dewetting of the bilayer. After bilayer deposition and before $I-V$ measurements, the ionic strength was brought back to 135 mM KCl both on top of and below the pore chip to keep the bilayer hydrated properly, and the current was measured through the tip holder using the conductance AFM setup. Once a proper seal was achieved by the bilayer, gramicidin (Sigma-Aldrich, St. Louis, MO), an ion-channel-forming peptide (dissolved in Milli-Q water with 135 mM KCl), was added to the buffer solution at a concentration of 0.2 mg/mL, and the current−voltage characteristics were measured as a function of time as gramicidin was inserted into the bilayer.

Results and Discussion

AFM imaging of initial test pores produced by electron beam lithography shows pores with a diameter ranging from 50 to 200 nm or more. An example of such nanopores is shown in Figure 3A. Large markers with a width of 500 nm (indicated by blue arrows in Figure 3) were used to find the patterns of interest by an optical microscope that is integrated with the atomic force microscope. After deposition of a lipid bilayer over the chip, the pores in the chip are covered by the bilayer. The larger corner markers (1 μm long) are still visible, possibly as the bilayers collapsed over such large openings due to a lack of sufficient stiffness to span the whole pore, allowing for easy navigation and as a reference to locate the nanopores under the bilayer (Figure 3A,B).

Figure 3B shows a lipid bilayer supported over the chip. The lipid bilayer covers most, if not all, of the pores in the underlying silicon nitride chip and also reveals several incomplete portions (holes, indicated by red arrows) of the bilayer. Such defects are common with adsorbing bilayers onto AFM substrates and were not created by the excessive AFM imaging force; force dissection of a bilayer requires a significantly larger AFM imaging force than used in this study.[14] The presence of a single lipid bilayer is confirmed by the thickness measurement along these holes. The AFM cross-sectional height measurements along one of these holes (Figure 3B, inset) shows a membrane thickness of ~5.5 nm, the nominal thickness of a common lipid bilayer.[14] The uniform thickness of the membrane over the whole silicon nitride nanochip (data not shown) suggests that only a single bilayer is adsorbed onto the chip.

Our aim here was only to ascertain whether we could image a bilayer over the pores in a supported bilayer system, a key requirement for the applicability of a supported bilayer system for the direct 3D structure and activity study of ion channels. Thus, examining the molecular structure of lipid head groups in the bilayer, though desirable, was beyond the scope of the present work and hence not undertaken.

Direct evidence that the bilayers are strong enough to be imaged while overlying nanopores in a silicon nitride chip was obtained: the lipid bilayers imaged with AFM show them spanning even a large 500 nm wide gap of the alignment marks in the silicon

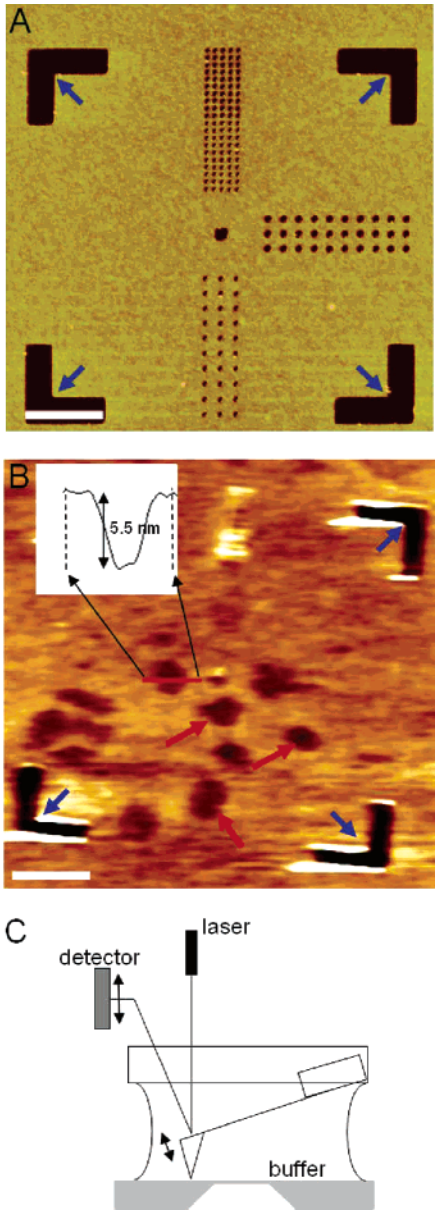

Figure 3. (A) Tapping mode AFM image of arrays of nanopores (z scale 10 nm). The pores are produced in a silicon nitride chip using electron beam lithography and range in size from 50 to 100 nm. (B) After deposition of lipid vesicles, the AFM image in PBS shows a bilayer covering the pores. The bilayer has several holes; the cross-section of a hole in the bilayer (inset) indicates a hole depth of 5.5 nm, the typical thickness of a lipid bilayer.[14] Scale bars represent 1 μm. Blue arrows indicate 1 μm long corner alignment marks, and red arrows indicate defects in the bilayer. (C) Schematic of the liquid cell AFM setup for imaging the silicon nitride chip and bilayer.

nitride chip. Figure 4 shows an example where a lipid bilayer is suspended over parts of an alignment mark, but ruptures in the other part (Figure 4B). Parts B, D, and F of Figure 4 show height images obtained in force−volume mode. Each pixel shows height information deduced from the extent of z travel necessary to deflect the cantilever by an amount that corresponds to a force of 1.5 nN. Force−distance curves are acquired simultaneously. The granular features resulted from the FIB ion milling of such large holes and were there before bilayer deposition. Most likely the bilayer was ruptured during its deposition and not during AFM imaging, since the remaining suspended part of the bilayer was imaged successively over several AFM scans. Significantly, even in these suspended bilayers, defects (holes) as shown in the

(17) Lin, H.; Zhu, Y. W. J.; Lal, R. *Biochemistry* **1999**, *38*, 11189−11196.

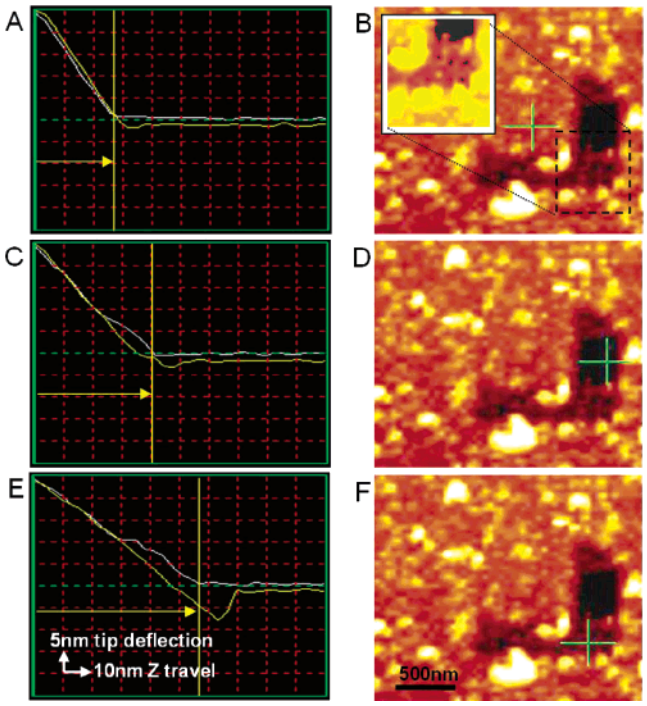

Figure 4. Relative stability of a lipid bilayer over a large nanopore. Force−distance curves acquired over various portions of lipid bilayers. Panels A, C, and E show typical force−distance curves, and panels B, D, and F show the position (green "+" signs) of the force curve taken on bilayers over the chip, an uncovered pore in an alignment mark, and a partially covered portion of the pore in the alignment mark, respectively. Panels B, D, and F are acquired using force−volume imaging (see the text for details). The increased *z* distance from the point of contact to preset deflection indicates a softer bilayer (yellow arrows). The inset in panel B shows a stable suspended bilayer imaged repetitively using a 1.5 nN force. The scale bar represents 500 nm, and the *z* scale is 2 nm.

bilayer over nanopores (Figure 3) are present. The inset in Figure 4B shows a suspended bilayer in more detail; the imaging force (∼1.5 nN) is low enough to have a stable membrane for repetitive imaging.

As further evidence for the rigidity of these suspended bilayers, we examined force curves and the relative stiffness of the membrane and the support chip. AFM force measurements over various regions of the same specimen show the relative stiffness of a bilayer on the silicon nitride membrane (Figure 4A), of a hole in the edge of an alignment mark without a bilayer (Figure 4C), and of a bilayer suspended over the opening (Figure 4E). The increased amount of *z* travel necessary to obtain the same cantilever deflection when the AFM tip is over the suspended bilayer vs for the bilayer on the silicon nitride substrate indicates that the bilayer is softer when suspended over the alignment mark hole and yet strong enough to be imaged with AFM. The inset in Figure 4B shows a suspended bilayer in more detail; the force−volume imaging force (∼1.5 nN) is low enough to have a stable membrane for repetitive imaging. The indication of a slightly softer surface at the edge of the hole is most likely caused by the AFM tip contacting the edge of the bilayer from the side.

We then examined whether the pores in the silicon nitride chips would allow electrical conductance in a defined medium. To minimize interference from neighboring pores as could occur in a chip with multiple pores (Figures 3 and 4), we designed chips with a single central pore with a diameter of 70 nm (Figure 1F). For measuring current through the nanopores in the chip, pores produced by FIB in silicon chips were used. The pores in the chip were insulated and shrunk in size by thermal oxide deposition using plasma-enhanced CVD. They do not contain the large alignment markers that would give rise to leakage current as is the case in our electron beam lithography produced pores, and only one pore is milled in each die. Furthermore, the FIB milling process is a direct one-step process, eliminating the need for photoresist or electron beam resist materials potentially contaminating the sample. To measure electrical conductance through a pore in the chip, a 135 mM KCl solution was used under the nitride membrane in the cell containing the bottom electrode, and the platinum-coated AFM tip was used as the second electrode. The same platinum-coated AFM tip was used for simultaneous imaging of the structures. To measure local conductance and not the bulk conductance through the complete cantilever holder, no buffer solution was used on top of the membrane and only humid air was gently flowed over the surface. This allowed maintaining a water meniscus between the tip and silicon chip and confined the measurement of conductance through the tip apex and not the rest of the cantilever holder assembly. Results of simultaneous AFM imaging and conductance measurements are shown in Figure 5.

The single pore in the silicon chip is imaged repeatedly using different bias voltages applied to the bottom electrode located under the silicon nitride membrane in 135 mM KCl buffer. The height image does not show the pore depth and size properly, and the pores appear shallow. This is caused by tip-induced broadening due to the large tip radius of the platinum-coated tips. The current images show bright spots where there is a current flowing between the bottom electrode and the tip. The "current spots" are larger than the pore, suggesting that the water layer (due to humidity) near the pores is conductive enough to allow current to flow and thus the current is not exclusively limited to the on-pore area only. Increasing the bias voltage applied to the bottom electrode under the pore chip from −0.5 to −1.0 V and subsequently to −2.0 V resulted in increases in the current from 5 to 65 pA and from 65 to 214 pA, respectively (Figure 5). These results indicate the suitability of the nanopore support system to detect ion channel conductance of 10 pS or lower with these AFM tip electrodes over large support pores. We have not measured the conductance over smaller silicon chip pores mimicking ion channels; designing chips with such small pores is beyond the scope of the present work. However, it is expected that the sensitivity of the conducting tips would be sufficient to measure ion channel conductance for small-diameter pores mimicking ion channels. Also, for such recordings, AFM tips would need to be coated with some other material, such as AgCl, to minimize charge buildup and current saturation.

We then recorded the electrical current across the chip pore after a lipid bilayer was adsorbed over the pore. Bilayers without any conducting pores would have a sealing effect over the chip nanopores, and hence, the conductance should be minimal. For such a study, lipid bilayers were formed by vesicular fusion. Lipid vesicles were deposited over the chips, and after 30 min (time that we have previously shown to form a bilayer from vesicular fusion[14,15]), the excess unadsorbed lipids and vesicles were rinsed away from the surface. Bulk electrical conductance across the supported chip nanopore and the overlying adsorbed lipid bilayer was measured using a drop of 135 mM KCl solution on top of the chip in which the AFM tip holder assembly was submerged and 135 mM KCl under the nitride membrane. The resulting $I-V$ curve was nearly flat, and the bulk electrical conductance across the bilayer was less than 0.025 nS (data not shown).

We then examined the possibility of using the chip nanopore to measure electrical conductance across ion channels recon-

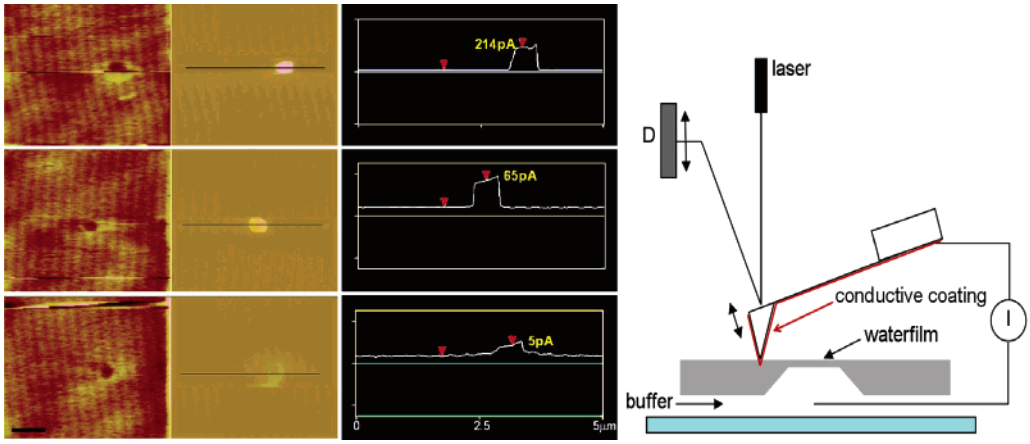

Figure 5. Combined AFM height (contact mode) and current imaging. The left images show the topography of the same FIB-milled pore imaged repeatedly with varying bias potential, −2.0 V (top), −1.0 V (middle), and −0.5 V (bottom). The right images are current images; a distinct current signal is observed over the pore. The amount of current is shown in the cross-sections of the current images, 214 pA at −2.0 V, 65 pA at −1.0 V, and 5 pA at −0.5 V. The right panel shows a schematic setup with the platinum-coated AFM tip as an electrode in buffer under the nitride window. The cantilever tip is coated with conductive titanium/platinum. The scale bar represents 1 μm. The z range is 10 nm (height image) and 250 pA (current image).

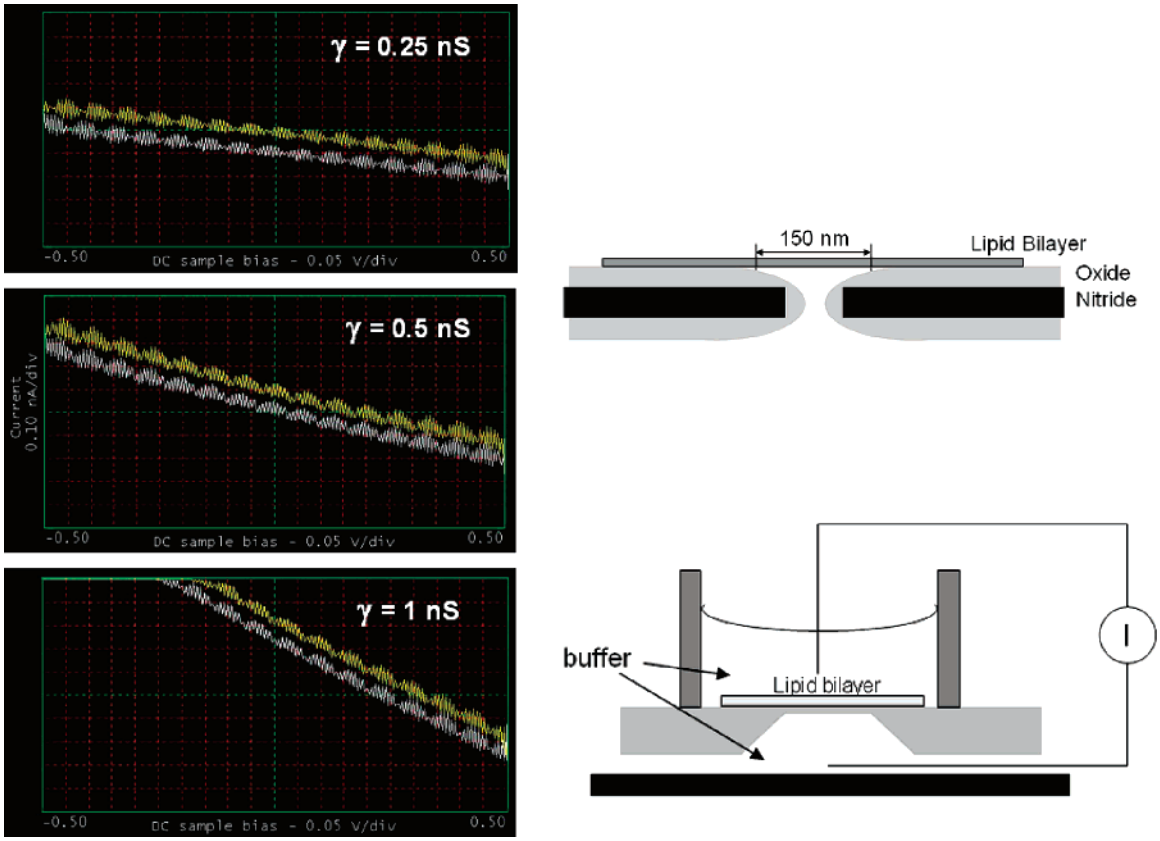

Figure 6. $I-V$ curves (left) collected 10 s (top), 2 min (middle), and 4 min (bottom) after addition of gramicidin to the lipid bilayer sample suspended over the nanopore. $I-V$ voltage range −0.5 to +0.5 V. Conductance increases from 0.025 nS (bilayer only) to 0.25, 0.5, and 1 nS, respectively. The right bottom panel shows a schematic setup, and the right top panel shows a schematic of the FIB-induced nanopore with deposited oxide and a bilayer.

stituted in the overlying lipid bilayer. As a preliminary measure, gramicidin (a known ion-channel-forming peptide) was added to the imaging solution at a concentration of 0.2 mg/mL. Gramicidin is known to form ion channels when inserted into a lipid membrane.[18,19] The effect of the online addition of gramicidin on the conductance across the bilayer and the underlying silicon nitride chip with the central pore is shown in Figure 6. Electrical conductance increased within seconds after online addition of gramicidin (Figure 6, top and middle left panels). During the gramicidin addition, no imaging was performed, eliminating the risk of puncturing the bilayer with the AFM tip. After 4 min of online addition of gramicidin, the electrical conductance stabilized at approximately 1 nS (Figure 6, bottom left panel). Since gramicidin is dissolved in the same

(18) Harms, G. S.; Orr, G.; Montal, M.; Thrall, B. D.; Colson, S. D.; Lu, H. P. *Biophys. J.* **2003**, *85*, 1826−1838.
(19) Busath, D. D.; Andersen, O. S.; Koeppe, R. E. *Biophys. J.* **1987**, *51*, 79−88.

water-based KCl solution as present above and below the bilayer, an increase in the conductance appears to be due to it forming ion channels in the bilayer membrane and not due to a solvent-induced leaky membrane. For comparison, as described above, no to very little electrical current was measured across the pure lipid bilayer or in the absence of other channel-forming proteins added to the bilayer. The conductance measured after online addition of gramicidin suggests that at least some of the gramicidin channels overlapped with the nanopore in the underlying silicon nitride membrane.

The conductance of a gramicidin ion channel is usually small, varies considerably, is dependent upon the solvent and membrane potential, and is influenced considerably by the nature of the detergents. Gramicidin channel conductances for 1 M NaCl and KCl have been reported to range from 10 to 17 pS.[19,20] Assuming a nominal single-channel conductance in the range of 10−20 pS, the number of functional gramicidin ion channels overlying the nanopore in the supported silicon nitride chip would be ∼50−100. No effort was made to measure single-channel conductance; this was beyond the scope of the present study. Our AFM tip with platinum coating would be subjected to capacitative saturation, and a tip with AgCl coating or with appropriate capacitative compensation would be needed for single-channel recording. Moreover, the density of gramicidin would need to be adjusted to yield a single or a few channels overlying the chip nanopore. Also no effort was made to image the 3D structure of individual ion channels; our only aim here was to ascertain whether the bilayer membrane would be strong enough for AFM imaging while overlying chip nanopores. For simultaneous high-resolution imaging and conductance measurements, one needs a sharp AFM tip (likely a nanotube) with the capability to measure *local* conductance in the fluid through the tip apex only. We have developed such a nanotube tip,[21] and with further development one would be able to accomplish the goal of simultaneous conductance/imaging studies at the single-ion-channel level. The main emphasis of the present work was to design an appropriate supported bilayer system and to examine its feasibility for AFM imaging and measuring current flowing through conducting pores reconstituted in an overlying lipid bilayer.

In summary, we report the design of a nanopore chip suitable for use as a support for lipid bilayer membranes with or without embedded channels and receptors wherein both sides of the extramembranous portions of these channels and receptors are accessible for online pharmacological and biochemical perturbations. The system allows for simultaneous AFM imaging and electrical recording and thus opens the possibility to study the direct structure−function relation of ion channels with high resolution: it will be possible to induce online gating of ion channels and image their 3D structural features in open and closed states while the ionic current passing through these channels is being recorded. With a further development of AFM tip technology that will allow for AFM tips that are conducting only at the final apex without the risk of contamination (as in wax-coated tips), this nanopore chip would allow for simultaneous molecular resolution imaging and single-channel electrical recording.

Acknowledgment. We thank Raymond Lee of FIB International for performing the focus ion beam milling procedure. The work was supported by grants from the NIH, California State Department of Health, and Philip Morris External Grant program.

LA062187Z

(20) Rokitskaya, T. I.; Kotova, E. A.; Antonenko, Y. N. *Biophys. J.* **2002**, *82*, 557A−557A.

(21) Chen, I. C.; Chen, L. H.; Ye, X. R.; Daraio, C.; Jin, S.; Orme, C. A.; Quist, A.; Lal, R. *Appl. Phys. Lett.* **2006**, *88*, 153102.